

AD-A162 191

APPLICATION OF MICROWAVE SPECTROSCOPY TO THE STUDY OF  
CORONAL FIELD CHANG (U) CALIFORNIA INST OF TECH  
PASADENA G J HURFORD MAR 85 SCIENTIFIC-1

1/1

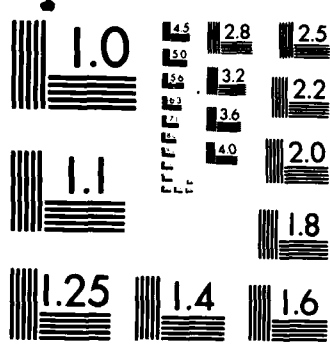
UNCLASSIFIED

AFGL-TR-85-0092 F19628-84-K-0023

F/G 3/2

ML





MICROCOPY RESOLUTION TEST CHART  
NATIONAL BUREAU OF STANDARDS-1963-A

12

AFGL-TR-85-0092

APPLICATION OF MICROWAVE SPECTROSCOPY  
TO THE STUDY OF CORONAL FIELD CHANGES  
ASSOCIATED WITH A DISAPPEARING SUNSPOT

G.J. Hurford

California Institute of Technology  
1201 E. California Blvd.  
Pasadena, CA 91125

March 1985

Scientific Report Number 1

Approved for public release; distribution unlimited

DTIC  
ELECTE  
DEC 10 1985  
S  
D

AD-A162 191

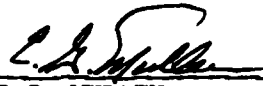
DTIC FILE COPY

AIR FORCE GEOPHYSICS LABORATORY  
AIR FORCE SYSTEMS COMMAND  
UNITED STATES AIR FORCE  
HANSCOM AFB, MASSACHUSETTS 01731

85 12 10 016

This technical report has been reviewed and is approved for publication.

  
E.W. CLIVER  
Contract Manager

  
E.G. MULLEN  
Branch Chief

FOR THE COMMANDER

  
R.C. SAGALYN  
Director  
Space Physics Division

This report has been reviewed by the ESD Public Affairs Office (PA) and is releasable to the National Technical Information Service (NTIS).

Qualified requestors may obtain additional copies from the Defense Technical Information Center. All others should apply to the National Technical Information Service.

If your address has changed, or if you wish to be removed from the mailing list, or if the addressee is no longer employed by your organization, please notify AFGL/DAA, Hanscom AFB, MA 01731. This will assist us in maintaining a current mailing list.

REPORT DOCUMENTATION PAGE

1a. REPORT SECURITY CLASSIFICATION <b>Unclassified</b>		1b. RESTRICTIVE MARKINGS	
2a. SECURITY CLASSIFICATION AUTHORITY		3. DISTRIBUTION/AVAILABILITY OF REPORT	
2b. DECLASSIFICATION/DOWNGRADING SCHEDULE		Approved for public release; distribution unlimited.	
4. PERFORMING ORGANIZATION REPORT NUMBER(S)		5. MONITORING ORGANIZATION REPORT NUMBER(S) AFGL-TR-85-0092	
6a. NAME OF PERFORMING ORGANIZATION Calif. Inst. of Technology	6b. OFFICE SYMBOL (If applicable)	7a. NAME OF MONITORING ORGANIZATION Air Force Geophysics Laboratory	
6c. ADDRESS (City, State and ZIP Code) 1201 E. California Blvd. Pasadena, California 91125		7b. ADDRESS (City, State and ZIP Code) Hanscom Air Force Base Massachusetts 01731 Monitor/Edward Cliver PHP	
8a. NAME OF FUNDING/SPONSORING ORGANIZATION	8b. OFFICE SYMBOL (If applicable)	9. PROCUREMENT INSTRUMENT IDENTIFICATION NUMBER F19628-84-K-0023	
8c. ADDRESS (City, State and ZIP Code)		10. SOURCE OF FUNDING NOS.	
		PROGRAM ELEMENT NO. 61102F	PROJECT NO. 2311
		TASK NO. 2311G3	WORK UNIT NO. 2311G3BJ
11. TITLE (Include Security Classification) (see reverse)			
12. PERSONAL AUTHOR(S) G. J. Hurford			
13a. TYPE OF REPORT Sci. Rep. #1	13b. TIME COVERED FROM 1/84 TO 12/84	14. DATE OF REPORT (Yr. Mo., Day) 1985 March	15. PAGE COUNT 15 18
16. SUPPLEMENTARY NOTATION			
17. COSATI CODES		18. SUBJECT TERMS (Continue on reverse if necessary and identify by block number)	
FIELD	GROUP	SUB. GR.	
			Microwave Spectroscopy, Sunspot, Coronal Magnetic Fields
19. ABSTRACT (Continue on reverse if necessary and identify by block number)			
<p>A critical physical parameter affecting solar activity is the distribution of coronal magnetic fields. Microwave observations provide the only technique for the quantitative measurement of these fields. This report presents the preliminary analysis of high spatial and spectral resolution observations designed to measure the distribution and evolution of the coronal magnetic fields of a disappearing sunspot.</p> <p>Data at 56 frequencies between 1.2 and 14 GHz were acquired with the three-element frequency-agile interferometer, of the Owens Valley Radio Observatory. This system directly measured the size of coronal microwave sources at each frequency and polarization. The temperature of the source was determined from the ratio of source flux to area. This</p>			
20. DISTRIBUTION/AVAILABILITY OF ABSTRACT UNCLASSIFIED/UNLIMITED <input checked="" type="checkbox"/> SAME AS RPT. <input type="checkbox"/> DTIC USERS <input type="checkbox"/>		21. ABSTRACT SECURITY CLASSIFICATION unclassified	
22a. NAME OF RESPONSIBLE INDIVIDUAL Edward Cliver		22b. TELEPHONE NUMBER (Include Area Code) (617) 861-3975	22c. OFFICE SYMBOL AFGL/PHP

Block 11: Application of Microwave Spectroscopy to the Study of Coronal Field Changes Associated with a Disappearing Sunspot (unclassified)

Block 20:

yielded the size and brightness temperature spectra of the microwave sources associated with a sunspot as it disappeared over three successive days.

On the basis of gyroresonance opacity, the corona would be expected to be opaque at microwave frequencies at surfaces corresponding to specific values of coronal field strength. The overall form of the observed spectra was consistent with such expectations, although there were differences of potential physical significance.

# APPLICATION OF MICROWAVE SPECTROSCOPY TO THE MEASUREMENT OF CORONAL FIELD CHANGES ASSOCIATED WITH A DISAPPEARING SUNSPOT

G. J. Hurford

264-33 Caltech  
Pasadena CA 91125

## I. INTRODUCTION

Coronal magnetic fields are intimately linked with most aspects of solar activity. Open field configurations are causally related to coronal holes; strong fields are associated with solar active regions; unstable coronal fields result in solar flares. Observations of coronal fields, however, have been based largely on soft X-ray images such as were taken on Skylab, which clearly showed the important role of magnetic loops in the physics of the solar corona. However, such images cannot measure the strength or the fields. Knowledge of the field strength and distribution is important since in solar active regions, the magnetic energy density greatly exceeds the plasma ("nKT") energy density.

Although indirect estimates of the coronal field strengths have been obtained by extrapolating from photospheric magnetographs, uncertainties in calibration and well-founded misgivings about the choice of appropriate magnetic field model limit the usefulness of this strategy. Microwave observations provide another approach. Under normal circumstances, the solar corona is optically thin at microwave frequencies, resulting in observed brightness temperatures of  $10^4$  to  $10^5$  K. In the presence of strong magnetic fields, however, gyroresonance opacity can render the corona optically thick so that coronal brightness temperatures are achieved at such locations. The corresponding sources have been observed by many workers with high resolution microwave imaging instruments such as the Very Large Array and the Westerbork interferometer.

Gyroresonance opacity is significant at frequencies which are low integral multiples of the local gyrofrequency. It is important to recall that the gyrofrequency,

$$\nu_g \text{ [GHz]} = 2.8 B \text{ [kg]} \quad (1)$$

depends only on the magnetic field, B, and is independent of electron temperature, density or velocity. At temperatures and densities typical of coronal conditions, gyroresonance

opacity usually provides significant optical depth at the 2nd and 3rd harmonics in the extraordinary propagation mode (left circular polarization for downward directed fields) and at the 2nd harmonic in the ordinary mode. The optical depth at higher harmonics is usually much less than 1 and so will be neglected here.

These considerations lead to the schematic picture illustrated in Figure 1, whereby at a fixed frequency, the coronal microwave emission above a sunspot is generated in magnetic shells, representing isogauss surfaces. At 5 GHz for example, the emission would come from shells where the magnetic fields are approximately 600 and 900 gauss. (At 600 and 900 gauss, the gyrofrequencies are 1.7 and 2.5 GHz, whose 2nd and 3rd harmonics are 5 GHz.) Thus at 5 GHz, the ordinary mode emission comes from a surface where the magnetic fields is 900 gauss, whereas the extraordinary mode emission comes from a 600 gauss shell. (In the extraordinary mode, the 900 gauss shell also would emit at 5 GHz, but such emission normally would be hidden under the opaque, 600-gauss shell.)

To imaging observations, these shells appear as localized areas coronal temperatures. Their diameters are determined by the intersection of the isogauss shells with the transition zone. (Emission by the shell below the transition zone is unimportant since even if it were optically thick, it could not have  $10^6$  K brightness temperature.) Note that at higher frequencies, the shells would correspond to stronger fields and so we would expect a decreased diameter. At the "transition" frequency corresponding to the shell which is tangent to the transition zone, we would expect that the diameter would approach zero and at frequencies above this cutoff, coronal brightness temperatures would not be achieved.

The variation of the diameter of these shells with frequency depends on the configuration of the magnetic field in the corona. Thus measurement of the diameter and temperature of these shells as a function of frequency can provide a direct, quantitative measurement of the magnetic field distribution in the corona. More detailed calculations illustrating these concepts are presented in such papers as Kruger, Hildebrandt and Furstenberg (1985).

This report outlines the initial results of measurements designed to measure the size and brightness temperature of these shells as a function of frequency.

## II. OBSERVATIONS

The observations were made with the frequency-agile interferometer at the Owens Valley Radio Observatory (OVRO). This system (Hurford, Read and Zirin 1984) can observe at up to 86 frequencies between 1 and 18 GHz in both right and left circular polarization. By rapidly switching among frequencies, detailed spectra can be obtained in a few seconds.

Early results (Hurford, Gary and Garrett 1985) used two antennas for measurements of active regions. With only a single baseline, it was not possible to directly measure the size of the sources. The resulting spectra were consistent, however, with the arguments advanced in Section I. Soviet workers (cf Akhmedov et al. 1983) have conducted corresponding multifrequency measurements between 7.5 and 15 GHz using their RATAN-600 instrument.

The present results are based on the first interferometric measurements using three antennas. As discussed below, the resulting three baselines permitting a direct measurement of source size. The east-west separation of the antennas was 0.183, 1.067 and 1.250 km with the central antenna displaced 0.032 km north of the line joining the outer two. The resulting resolution (fringe spacing) was inversely proportional to frequency (with a value of 10 arcsec at 5 GHz), and was sufficient to resolve the sources at each frequency. Although data were acquired at 86 frequencies between 1 and 18 GHz, but the analysis discussed here will be limited to 56 frequencies between 1.2 and 14 GHz, a restriction which is not important for our present purposes.

The limited field of view afforded by the use of large antennas (27 and 40 m diameter paraboloids) made it possible (at all but the lowest frequencies) to restrict the field of view to a single active region. The observing procedure consisted of sequencing among one or more active regions with dwell times of 10 to 90 minutes on each. Several times during the day, a calibrator source (3C84 or 3C273) was observed for about 20 minutes.

The present report will be confined to the first 3 of 6 consecutive days of observations of AR4549. The H-alpha appearance of this region on the first day (July 26, 1984) is shown in Figure 2 where it is seen to be dominated by a single sunspot. Between July 26 and 28, the spot progressively weakened. We shall be interested therefore not only in the coronal field distribution, but also in how this distribution evolved as the spot disappeared.

### III. DATA ANALYSIS

The fundamental calibration required is that of the interferometer amplitudes as a function of polarization, baseline and frequency. This calibration was based on extended observations of 3C373 and 3C84. Solar amplitudes were then calibrated by direct comparison with the amplitudes observed on these calibrators. Noise sources internal to each receiver were used to correct for small day to day variations in gain. The resulting calibrations are estimated to be good to about 10%, with a principal source of uncertainty being our imperfect knowledge of the calibrator spectra.

During the course of each day, the observed amplitudes and phases varied as the rotation of the earth changed the projected baseline (viz, the length and orientation of the baseline as seen from the perspective of the source). These variations, which had the expected qualitative form, can be exploited to make a crude map of the source at each frequency. Such mapping, however, is beyond the scope of this report. Therefore we further restrict the analysis to data acquired in a ~20 minute period each morning, a restriction that will still enable us achieve our objective of measuring the size and brightness temperature spectra. The use of a common time of day minimizes potential systematic errors introduced by the neglect of the details of the source structure.

The fundamental data reduction task consisted of automated editing of the data to remove periods of phase-lock anomalies or marginal antenna tracking and intervals during which the receivers were changing frequency or polarization. The data were then sorted by frequency/polarization, and corrections made for the calculated effects of baseline errors, earth and solar rotation. Amplitudes and phases were then vector-averaged over the chosen ~20 minute period, and the amplitudes calibrated as discussed above.

This procedure yielded fully calibrated amplitudes and partially calibrated phases on each of 3 days for each of 3 baselines at 56 frequencies in both right and left circular polarization. The optical data showed a region dominated by a single sunspot. Therefore a single microwave gyroresonance source was expected as well. This hypothesis was tested by forming the closure phase (Pearson and Readhead, 1984) at each frequency and polarization. Closure phase can be defined as the sum of the three phases observed on each baseline. Such a closure phase has the property that its value is independent of antenna-based calibration errors (viz, calibrated phases need not be used to form the sum). Its usefulness here is derived from the fact that the closure phase should be zero for the expected small, single, symmetrical source. For the more complex sources typical of

circumstances where free-free opacity becomes important, this would not necessarily be the case. Thus at each frequency, the closure phase represented a convenient, objective parameter which provides a measure of the importance of gyroresonance opacity. Frequencies and polarizations for which the closure phase did not come within  $\pm 1$  radian of the expected value were excluded from further analysis.

To determine the size of the source at each frequency/polarization, we assume a Gaussian profile and note the dependence of amplitude,  $A$  [Jy], on projected baseline,  $L$  [kml], for a Gaussian source of FWHM diameter,  $D$  [arcsec], observed at frequency,  $\nu$  [GHz]:

$$A = A_0 \exp -9.3 \cdot 10^{-4} (LD\nu)^2 \quad (2)$$

where  $A_0$  [Jy] is the limiting amplitude at  $L = 0$ , corresponding to an unresolved source. Thus a plot of  $\ln(A)$  vs  $L^2$  should be a straight line whose slope yields the value of  $D$ , the source diameter. A typical plot of this type, shown in Figure 3, shows that the diameter can be measured to an accuracy of about 5%. It might be noted that a principal source of calibration uncertainty, the flux of the calibrator, does not affect the measurement of this slope since all three points would be affected by the same error factor.

Having measured the diameter and  $A_0$ , the corresponding brightness temperature is given by the ratio of source flux to area, using the relation,

$$T_b = 3.5 \cdot 10^8 A_0 (D\nu)^{-2} \quad (3)$$

The resulting size and brightness temperature spectra for July 26 are illustrated in Figure 4. Figure 5 shows the evolution of these quantities over three successive days.

#### IV. RESULTS

Considering first the overall features of the spectra shown in Figure 4, for the LCP brightness temperature we note that coronal values above  $10^8$  K are maintained up to  $\sim 12$  GHz, where the temperatures drop rapidly to a few times  $10^7$  K. This is consistent with our expectation that the brightness temperature of the source would drop rapidly at the "transition" frequency where the corresponding isogauss shell was tangent to the transition zone. We also note that at lower frequencies, the source size decreases as frequency increases. The relatively constant value of source size above  $\sim 10$  GHz is not understood at present, but could be related to spatial fragmentation of high frequency sources

such as observed by Lang et al.(1983) at 15 GHz.

Comparing the RCP and LCP brightness temperature spectra, we note that the same qualitative behavior is observed in RCP as in LCP. Of particular interest is the fact that shifting the RCP spectrum up in frequency by a factor of 3/2 provides a reasonable agreement with the LCP brightness temperature spectrum. This is consistent with the choice of the 2nd and 3rd harmonics as the relevant values for the ordinary and extraordinary modes respectively.

A scaled comparison of the RCP and LCP size spectra might also be expected to behave similarly. Although they are in fact consistent in terms of the size and scaled frequency at which the size levels off, the RCP results at lower frequencies seem significantly higher than expected on the basis of the LCP spectra.

An unexpected feature noted in the brightness temperature spectra below the transition frequency is the apparent systematic increase from 2 to  $4 \cdot 10^6$  K as frequency increases. The significance of this feature in terms of the physics of the coronal fields is not clear.

The evolution of the coronal field as the sunspot disappeared is illustrated in Figure 5. Assuming that the 3rd harmonic is the relevant one in the extraordinary mode, from the brightness temperature spectra, it is apparent that the maximum field at coronal levels decreased from about 1300 to 1000 to 600 g over a two day period. The relatively modest change in the size spectra at the lower frequencies over this period is also significant. It may suggest that the weaker fields were not affected by the spot's disappearance to the same extent as were the stronger fields.

Another interesting facet to the field evolution was the systematic decline in brightness temperature associated with the strongest fields on each day, from 4 to 2 to  $1 \cdot 10^6$  K.

## V. DISCUSSION

The observations presented above represent preliminary analyses of the first interferometric size and brightness temperature spectra of an active region. The region selected for this analysis was deliberately chosen to be a simple one, a single isolated sunspot. In broad terms, we have seen that the spectra matched expectations based on straightforward application of gyroresonance effects, as exemplified in terms of magnetic shells. We have also seen that there are some aspects of the spectra that are not yet

understood. With more sophisticated analyses and interpretations, they too may yield their secrets.

At this preliminary stage of the analysis, it is inappropriate to consider detailed interpretations of the data in terms of the solar coronal fields. Nevertheless, it may be worthwhile to review the strengths and weaknesses of microwave spectroscopy (as we now understand them) for the measurement of such fields.

Unlike photospheric magnetograms which measure magnetic FLUX, (averaged over the seeing-dependent instrumental resolution), microwave spectroscopy measures magnetic FIELD in the corona. (Thus the present data are inconsistent with a model in which much of the coronal field is concentrated in small bundles of intense field as has been suggested at photospheric levels.) Through equation 1, the field measurements are inherently calibrated so that long term comparisons are quite feasible. Measurements such as these can be made in a few seconds, so that evolution on short time scales can be studied also. Full calibration of the phases will enable the location of the fields to be determined interferometrically to arcsecond accuracy.

The use of microwave spectroscopy for the measurement of coronal fields has some clear weaknesses. As our model suggests, the magnetic measurements represent emission coming from a range of heights, characterized by temperature, not distance above the photosphere. Furthermore, there are potential sources of ambiguity related to the specification of the appropriate harmonic, particularly for magnetic fields directed close to the line of sight. Perhaps the most serious weakness, however, is that with a three-element interferometer, there are serious limitations as to the morphological complexity of active regions which can be effectively studied. This problem cannot be resolved without the addition of more antennas.

In the near future with presently available instrumentation, we can anticipate the achievement of one-dimensional multifrequency synthesis maps of simple unipolar or bipolar regions; more sophisticated solar interpretations and modelling comparisons; studies of active region growth as well as decay; measurements of height dependence of magnetic fields (from limb observations) and application to studies of the magnetic fields of flaring loops.

In summary, the present analysis suggests the potential of microwave spectroscopy to provide quantitative measurements of the magnetic field distribution in the active solar corona.

### ACKNOWLEDGEMENTS

I am grateful to Dan Daugherty and to other members of the staff at Owens Valley for their assistance with this program. Dr. D. E. Gary, Dan Briggs and Margaret Liggett have made important contributions to the software and data analysis. The scientific guidance and encouragement of Dr. H. Zirin has been much appreciated.

Support for the solar observing program at Owens Valley and additional funding for data analysis is provided by the NSF under grants AST-8315217 and ATM-8309955 respectively.

AFGL support was provided under contract F19628-84-K-0023.

### REFERENCES

- Akhmedov, Sh. B., Gelfreikh, G. B., Furstenberg, F., Hildebrandt, J., and Kruger, A.: 1983, Solar Physics 88, 103.
- Hurford, G. J., Read, R. B., and Zirin, H.: 1984, Solar Physics 94, 413.
- Hurford, G. J., Gary, D. E., and Garrett, H. B.: 1985, "Radio Stars" (R. M. Hjellming and D. M. Gibson, eds.), D. Reidel, p379 (in press).
- Kruger, A., Hildebrandt, J., and Furstenberg, F.: 1985, Astron. Astrophys. 143, 72.
- Lang, K. R., Willson, R. F., and Gaizauskas, V.: 1983, Astrophys. J. 267, 455.
- Pearson, T. J., and Readhead, A. C. S., 1984: Ann. Rev. Astron. Astrophys. 22, 97.

Accession For	
NTIS CRA&I	<input checked="" type="checkbox"/>
DTIC TAB	<input type="checkbox"/>
Unannounced	<input type="checkbox"/>
Justification	
By .....	
Distribution /	
Availability Codes	
Dist	Availability for Special
A-1	

## FIGURE CAPTIONS

Figure 1: Schematic illustration of magnetic field lines above an isolated sunspot. The isogauss contours for 450, 600 and 900 gauss are shown. The 4th, 3rd and 2nd harmonics of the local gyrofrequency at these values respectively are equal to 5 GHz.

Figure 2: H-alpha filtergram from Big Bear Solar Observatory for AR4549 on 26 July 1984 when the region was located at S17E07.

Figure 3: A typical plot showing the dependence of observed amplitude (circles) on projected baseline. Gaussian sources of different FWHM diameters would yield lines with the slopes as indicated. In this case the source FWHM diameter is 8.8 arcseconds.

Figure 4: Size (top) and brightness temperature (bottom) spectra in LCP and RCP respectively, as observed on 26 July 1984.

Figure 5: Evolution of the LCP (extraordinary mode) size (top) and brightness temperature (bottom) spectra as the sunspot disappeared. Data acquired on July 26, 27 and 28 are represented by 0, 1 and 2 respectively. With the assumption that the 3rd is the highest optically thick harmonic, the frequency scale can be interpreted in terms of the magnetic field scale inserted at the top.

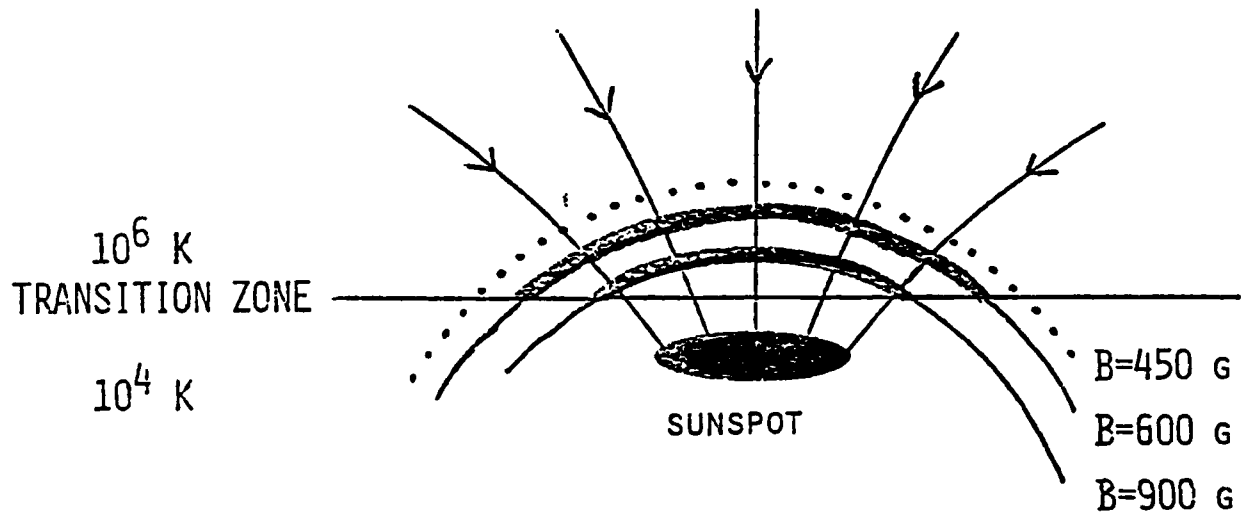


Figure 1



13

Figure 2

log(AMPLITUDE) vs BASELINE\*\*2 5 GHz LCP

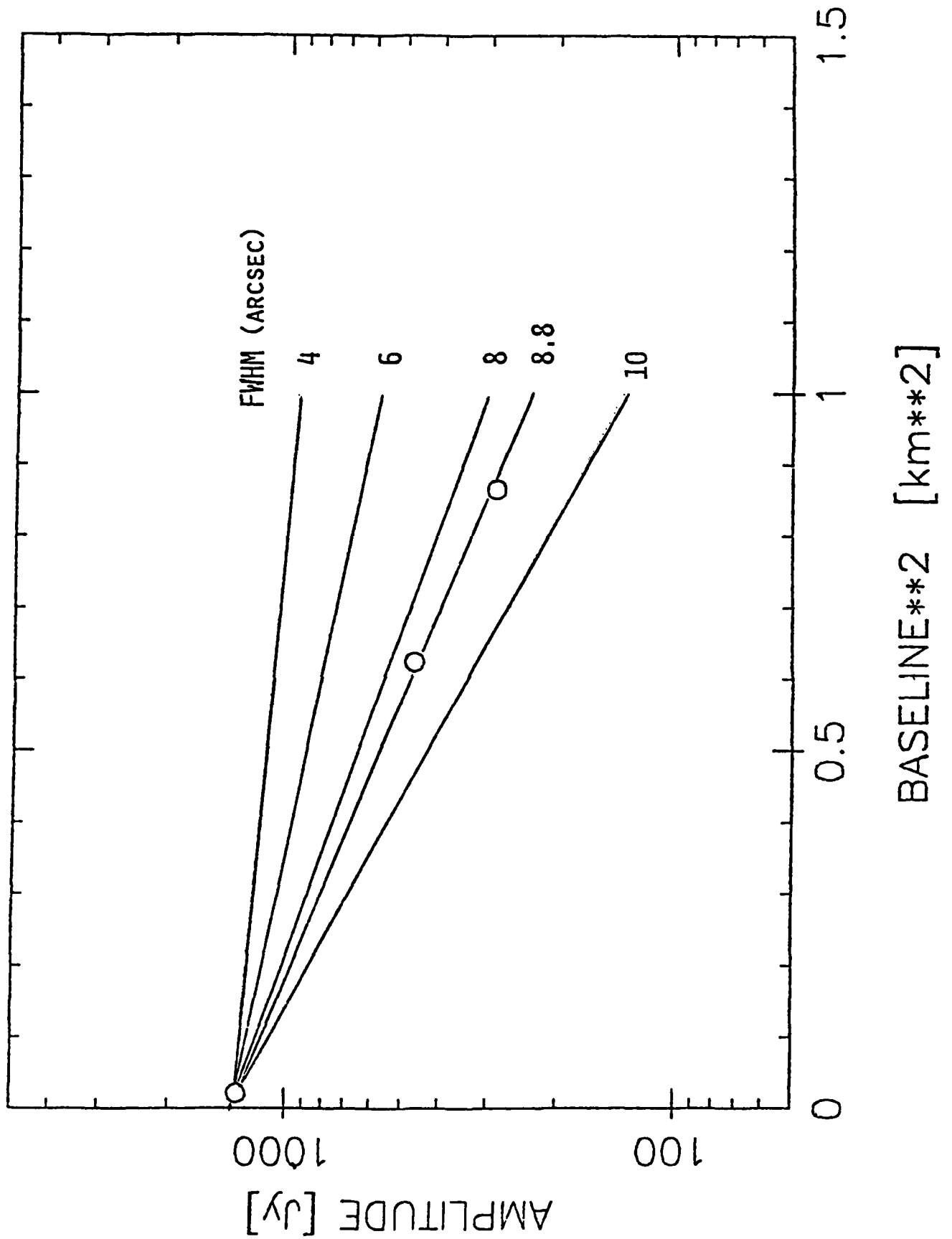
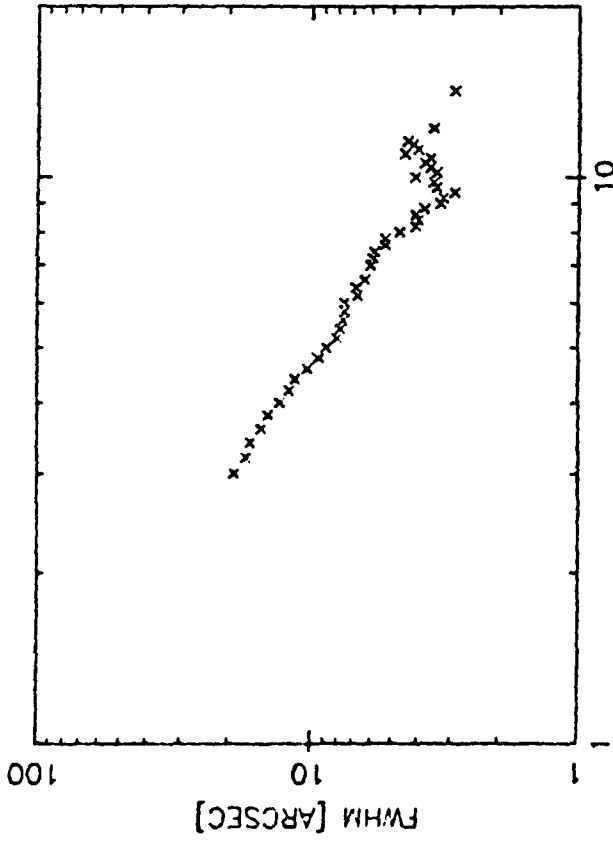


Figure 3

LCP SIZE SPECTRUM 84JUL26



RCP SIZE SPECTRUM 84JUL26

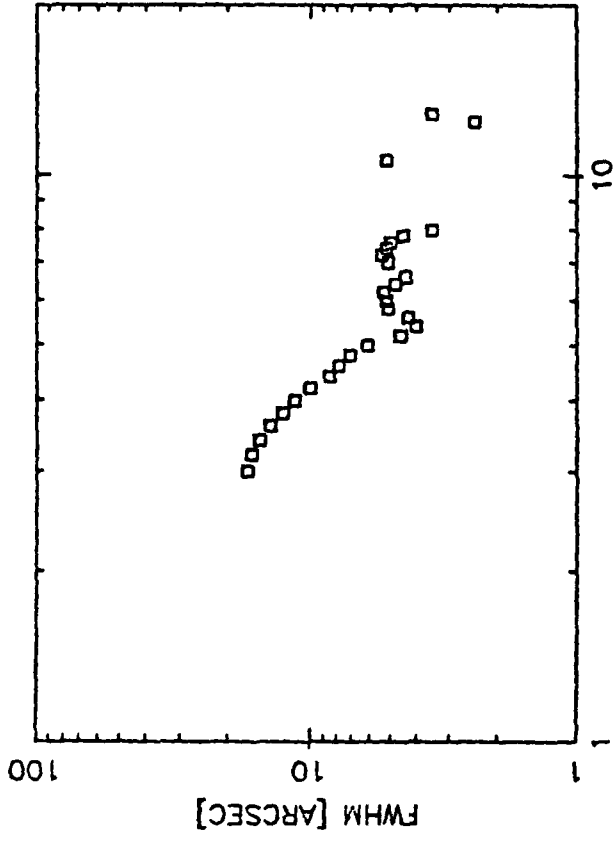
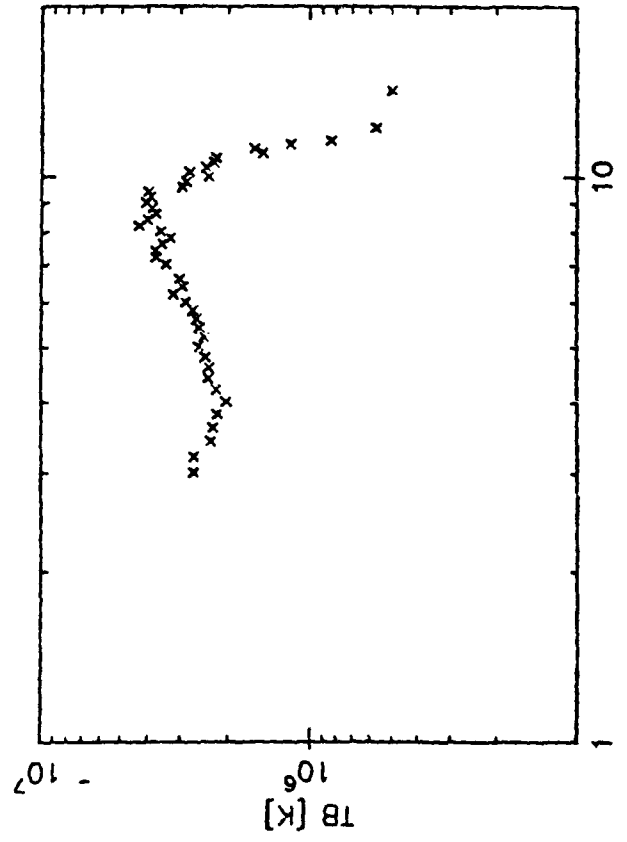
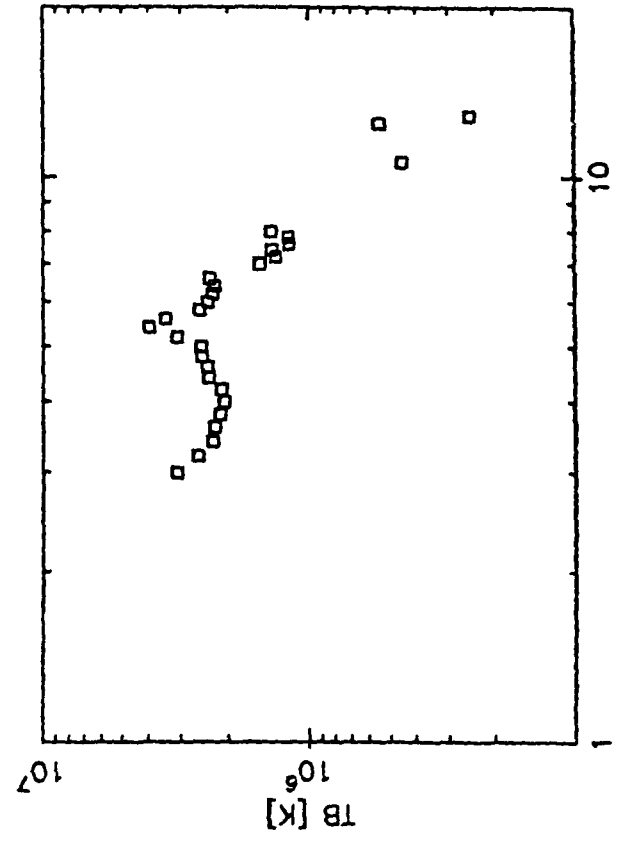


Figure 4

LCP BRIGHTNESS TEMPERATURE SPECTRUM 84JUL26



RCP BRIGHTNESS TEMPERATURE SPECTRUM 84JUL26





**END**

**FILMED**

---

*1-86*

**DTIC**